Annals of Biomedical Engineering, Vol. 47, No. 2, February 2019 (© 2018) pp. 335–353
https://doi.org/10.1007/s10439-018-02158-0

Stereotactic Systems for MRI-Guided Neurosurgeries: A State-of-the-Art Review

YUE CHEN,[1] ISURU GODAGE,[2] HAO SU,[3] AIGUO SONG,[4] and HONG YU[5]

[1]Department of Mechanical Engineering, University of Arkansas, Fayetteville, AR, USA; [2]School of Computing, DePaul University, Chicago, IL, USA; [3]Department of Mechanical Engineering, City College of New York, New York, NY, USA; [4]School of Instrument Science and Engineering, Southeast University, Nanjing, People's Republic of China; and [5]Department of Neurological Surgery, Vanderbilt University, Nashville, TN, USA

(*Received 25 August 2018; accepted 17 October 2018; published online 30 October 2018*)

Associate Editor Daniel Elson oversaw the review of this article.

Abstract—Recent technological developments in magnetic resonance imaging (MRI) and stereotactic techniques have significantly improved surgical outcomes. Despite the advantages offered by the conventional MRI-guided stereotactic neurosurgery, the robotic-assisted stereotactic approach has potential to further improve the safety and accuracy of neurosurgeries. This review aims to provide an update on the potential and continued growth of the MRI-guided stereotactic neurosurgical techniques by describing the state of the art in MR conditional stereotactic devices including manual and robotic-assisted. The paper also presents a detailed overview of MRI-guided stereotactic devices, MR conditional actuators and encoders used in MR conditional robotic-assisted stereotactic devices. The review concludes with several research challenges and future perspectives, including actuator and sensor technique, MR image guidance, and robot design issues.

Keywords—Stereotactic neurosurgery, Medical robot, MR conditional, Image-guided therapy.

INTRODUCTION

Stereotactic neurosurgery is a minimally invasive surgical procedure that uses 3-dimensional image guidance techniques and tools to assist surgeons in the localization of surgical targets in the brain. The first experimental stereotactic neurosurgery employed an orthogonal frame to insert an electrode into the cerebellum of an animal.[21] After 40 years, utilizing a custom-designed stereotactic apparatus, stereotactic thermocoagulation in thalamus was performed on a human.[84] In 1949, Lars Leksell developed an arc-radius stereotactic frame system with skull pin fixation; a system that's still widely used today.[54]

In the early years of stereotactic neurosurgery, visualization of structures within the brain was a major challenge.[41] The advent of computed tomography (CT) in the 1970s provided substantial improvements in the visualization of intracranial structures. In addition, the advances in mathematics and physics enabled accurate, efficient and safe stereotactic treatment, which led to clinical acceptance by the surgeons.

Surgeons and engineers continued to refine the existing designs and stereotactic methods to improve the outcome of stereotactic neurosurgeries. Magnetic resonance imaging (MRI), invented in the late 1970s, provided even more spatial resolution of visible structures within the brain.[62] The current stereotactic neurosurgery techniques consist of three basic components: stereotactic equipment, anatomic knowledge, and image guidance. Modern stereotactic neurosurgery utilizes preoperative CT/MRI to identify targets and calculate the desired linear trajectory to reach the target. Stereotactic neurosurgery is currently used in a myriad of procedures including electrode implantation, deliver ablative energy, brain tumor resection, *etc*.

Integration of minimally invasive robotics in neurosurgery improves precision and dexterity. These robotics could also benefit from the advantages of brain tissue deformation compensation capability (both whole brain tissue[26] and local brain tissue[64]) achieved by using the intraoperative image fusion. In addition, robotics also facilitates achieving higher level control constraints such as maximum spatial displacement and speed, to enhance safety. The first robotic neurosurgery was performed in 1985, which utilized an industrial robot (PUMA 200) to hold a stereotactic

Address correspondence to Yue Chen, Department of Mechanical Engineering, University of Arkansas, Fayetteville, AR, USA. Electronic mail: yc039@uark.edu

biopsy needle under CT-guidance.[49] Following this pioneering work, a number of robots were developed for neurosurgery, including the Minerva system,[27] CyberKnife,[1] Robot-Assisted Microsurgical System (RAMS),[52] SteadyHand,[94] Evolution 1,[102] NeuroMate,[98] NeuRobot,[40] Pathfinder,[24] SpinAssist,[57] and Neuroscience Institute Surgical System (NISS).[8] Figure 1 outlines the major technological milestones in the robotic-assisted stereotactic neurosurgery.

Apart from aforementioned CT-guided stereotactic robots, Masamune *et al.*, reported an MR conditional (definition of MR conditional is provided in "Terminology" section) robot to perform biopsies.[61] MRI provides excellent soft tissue resolution and superior image contrast without any radiation exposure. MRI could localize lesions that are not visible in CT images. Moreover, MRI has the intrinsic capability to visualize temperature at a target region that can be used to monitor ablation therapy.[20]

Despite these clinical advantages, implementation of MR-guided neurosurgery remains a technical challenge. The confined in-bore space of MRI scanners creates limited. In addition, MRI scanners produce strong magnetic fields and preclude the use of ferro- and para-magnetic materials. Electromagnetic interference (EMI) generated from the conventional surgical devices can also degrade MR image quality.[62] Radio frequency energy produced by the scanner can cause unsafe heating of surgical tools. As a result, overcoming the design and implementation challenges associated with MR conditional stereotactic devices are of paramount importance for MRI-guided stereotactic neurosurgery.

In this paper, we review the state of art MR conditional stereotactic neurosurgical devices. The paper is arranged as follows. Section "State-of-the-Art Neurosurgical Stereotactic Devices" presents the state-of-art review of the MR conditional stereotactic devices classified according to their functions. Section "Actuator and Sensor of MR Conditional Robot" describes MR conditional actuators and sensing technologies available for neurosurgical robots, followed by future directions in "Future perspectives" section, and conclusions in "Conclusions" section, respectively.

Terminology

Due to the widespread use of MR scanner, the U.S. Food and Drug Administration (FDA) defined the following terminology to clarify medical devices that can be used inside the MR room in 1997 and revised the terminology in 2005. The first terminologies proposed in 1997,[82] **MR safe** and **MR compatible**, are commonly used incorrectly since they were used without listing the detailed specific conditions, forming an impression that the device is MR safe/compatible in all the environments. The new terminologies proposed by American Society for Testing and Materials (ASTM) in 2005 and recognized by the FDA are defined as follows[2]:

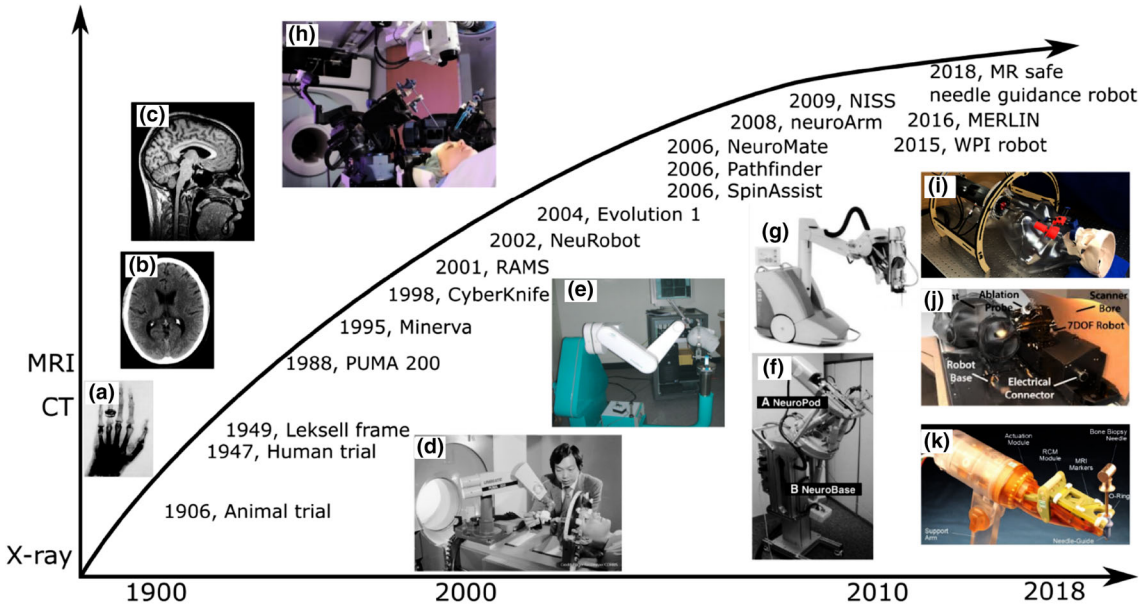

FIGURE 1. Some of the key technological breakthroughs in robotic-assisted stereotactic neurosurgery. Y-axis is the imaging modalities for image guided therapies (a: X-ray; b: CT; c: MRI). Image of (d) PUMA robot,[95] (e) NeuroMate,[98](f) NISS,[8] (g) Evolution 1,[102] (h) neuroArm (Courtesy of neuroArm Project, at University of Calgary), (I) MERLIN: MRI-Enabled Robotic non-Linear Incisionless Neurosurgery, (j) WPI neuro robot,[69] and (k) general MR safe needle guidance robot.[89]

MR safe: an object or device poses no known hazards in ***all*** MRI environments.

MR conditional: an object or device that has been demonstrated to pose no known hazards in a specified MRI environment with specified conditions of use.

MR unsafe: an object or device that is known to pose hazards in ***all*** MRI environments. The terms "MR safe" and "MR unsafe" are two extremes. To be qualified for the MR safe requirement, more scientifically based rational needs to be provided instead of test data. Although both the prior terminology and the latest terminology are still coexisted, we replace the term "MR compatible" by "MR conditional" in this review paper to avoid confusions for future readers.

STATE-OF-THE-ART NEUROSURGICAL STEREOTACTIC DEVICES

This section reviews the manual and robotic-assisted systems used in MRI-guided neurosurgeries according to their clinical applications, namely laser ablation, electrode implantations, biopsy, microsurgery, and aspiration, *etc*. The key features of each system are summarized in Table 1. Robotic platforms for neurosurgeries guided by CT/Ultrsound/Fluoroscopy are not covered in this review paper since these have been extensively reviewed in a number of recent publications.[25,58,80,83,101]

MRI-Guided Laser Interstitial Thermal Therapy (MRgLITT)

Image-guided laser ablation has been gaining attention for localized treatment of neurologic disorders, such as brain tumor and epilepsy resection.[63] It was proposed by Bown[5] in 1983 and underwent human trial for treatment of deep-seated brain tumors in 1990.[91] Thermal therapy is a treatment option for the patients who do not qualify for surgical resection due to target location. During thermal therapy, target tissue is heated to 46°–60°, thereby producing cell death. MRI thermography provides real-time temperature monitoring, thus maintaining the accuracy and effectiveness of MR-guided thermal therapy.[68] In this sec-

TABLE 1. Summary of the state-of-the-art MR conditional stereotactic aiming systems.

Project	Phase	Group	Purpose	Features	Sources
NeuroBlate	FDA approved	Monteris Medical Inc.	Thermal therapy	Real-time image guidance Manual control	97
Visualase	FDA approved	Visualase Inc.	Thermal therapy	Relies on Leksell frame and cranial anchor for probe targeting Manual control	99
MERLIN	Phantom test	Vanderbilt	Thermal therapy	Transformenal approach Nonlinear trajectory Pneumatic motor actuated	23
WPI robot	Phantom test	WPI	Thermal therapy	8 degrees of freedom Piezo motor actuated	56
SMA robot	Phantom test	UMD	Thermal therapy	Actuated by shape memory alloy	39
Nexframe	FDA approved	Medtronic Inc.	Electrode placement	Real-time image guidance Manual control	86
Clearpoint	FDA approved	MRI Interventions Inc.	Multiple purposes: Thermal Therapy biopsy and electrode placement	Intraoperative image guidance In-scanner remotely manual control	85
neuroArm	Submitted FDA 510 K	IMRIS Inc.	Microsurgery	Two 7-DoF robotic arms 1st MR conditional neurosurgical robot tested in patient study Ultrasonic motor actuated	93
ICH robot	Phantom test	Vanderbilt	Intracerebral hemorrhage debulking	Concentric tube approach Real-time MRI guidance Pneumatic motor actuated	15
Biopsy robot	Phantom test	Uni of Tokyo	Biopsy	High accuracy 1st MR conditional robot Ultrasonic motor actuated	61
Needle guidance robot	*In vitro* test	JHU	Multiple purpose including neurosurgery and bone biopsy	MR safe robot powered with pneumatic stepper motor High accuracy Multiple purpose	44

tion, we will review the state-of-the-art stereotactic devices that are developed for MRgLITT.

NeuroBlate® System

The NeuroBlate® system (Monteris Medical Corporation, Plymouth, MN) received FDA 510(k) clearance in 2009 for brain tumor ablation treatment (Fig. 2). The ablative energy delivery system consists of a ϕ 3.2 mm CO_2 cooled laser probe integrated with a thermal couple to provide temperature feedback. The AXiiiS stereotactic aiming device was developed based on the 3-RPR (rotational-prismatic-rotational) parallel manipulator working principle, which consists of three variable length supporting legs. Once the AXiiiS aiming device is fixed to the patient's skull with MR conditional screws, its orientation can be modified by loosening the clamp of each ball joint and changing the length of each leg. To perform MRgLITT with the NeuroBlate® system, the patient's head is rigidly fixed with respect to the immobilization frame throughout the therapy using MR conditional pins. MR imaging of the patient's head and immobilization frame is performed and this imaging data is used for target localization, entry point identification, and laser probe depth calculation. After the burr hole is created and dura is opened at the planned entry point, the laser probe is inserted manually through the aiming device bore. Following MRI acquisition to verify the ablation probe position, MR thermography images around ablation probe tip are obtained throughout laser energy delivery to monitor the treatment outcome in real-time.

Noteworthy features of the NeuroBlate® platform is its 'side-fire' capability, which delivers the ablation energy from the probe side. That the laser energy can be generated from the side of ablation probe Having this advantage could compensate the potential probe insertion error since firing the probe in a specific direction for long time can result in larger ablation area in that direction. This capability avoids multiple insertion processes occurred in the conventional therapies in order to cover the large targeted ablation zone.[65] Noting that the NeuroBlate® frame can also be integrated with a customized 3D printed aiming frame (STarFix microTargeting™, FHC microTargeting platform, ME, USA) for MRI-guided ablation therapy,[6] which could results in the benefit of shortening operation procedure time and extensive planning prior to the surgery.

Visualase System

The Visualase® Thermal Therapy System (Visualase, Houston, TX) is another commercially available product.[99] It is a portable cart consisting of the laser energy delivery system, MR conditional laser probe applicator, peristaltic cooling pump, and navigation/visualization system. The pre-LITT preparation process is similar to that of the NeuroBlate®-based approach, including the anesthesia, target identification, and entry point selection *etc*. A stereotactic frame is used to guide the drill at the planned entry site and along the planned trajectory for burr hole creation (Fig. 3). A plastic cranial anchor is then screwed to the burr hole. The laser probe is then inserted through the cranial anchor to the target position. The insertion length is calculated through navigation software. The stereotactic frame is removed after the preparatory work is finished[96] and the patient is transported to the MR room. A surgeon controls the ablation system remotely under intraoperative MR temperature feedback guidance.

A noteworthy advantage of the Visualase® system compared to the NeuroBlate® system is that it could be potentially faster in creating the same ablation zone.

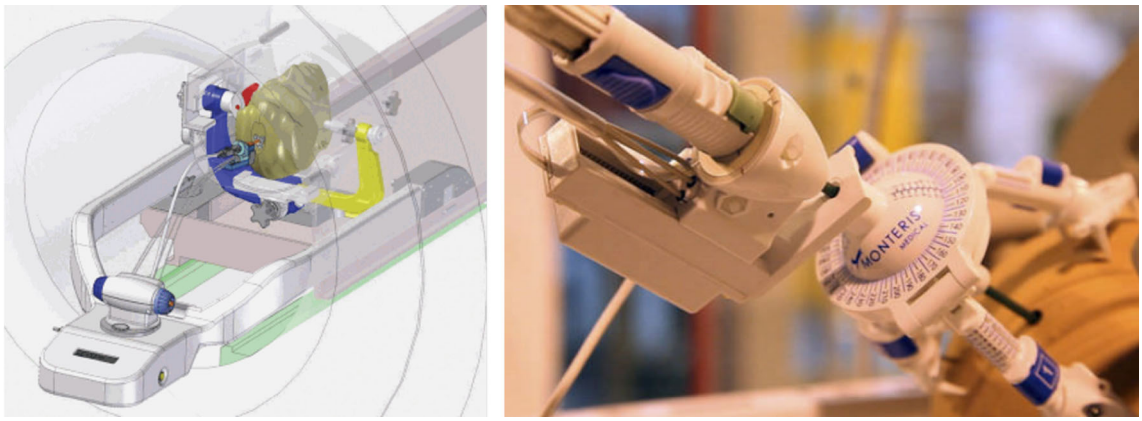

FIGURE 2. Left: NeuroBlate® systemmounted on the patient head model inside MRI scanner.[97] The surgeon operates the handheld controller to control laser probe. Right: The AXiiiS® Stereotactic aiming device mounted on the patient's head.

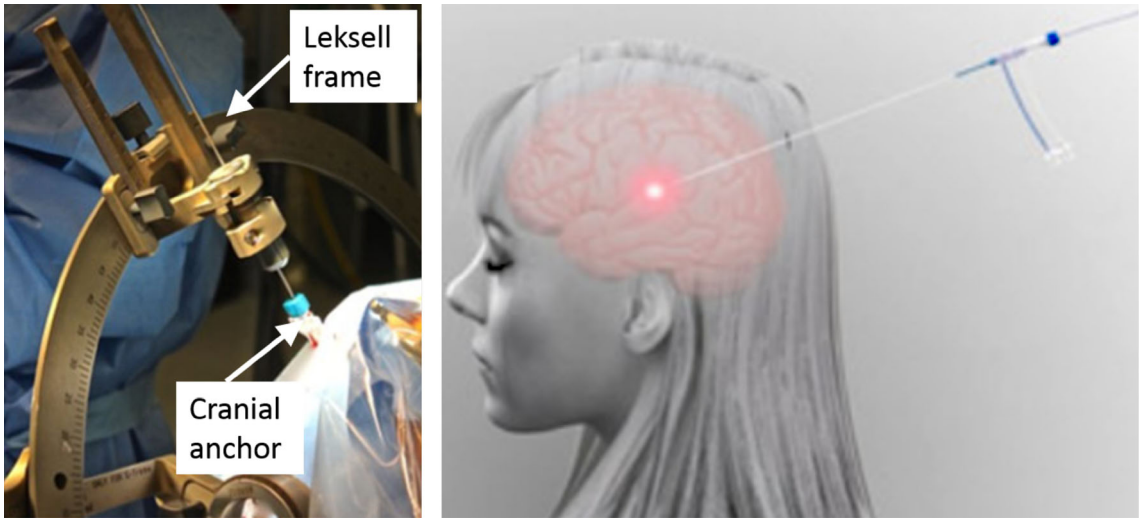

FIGURE 3. Left: Stereteotactic placement of a plastic cranial anchor guided by Leksell frame at desired orientation for Visualase® based laser ablation.[96] Right: Schematic diagram of the laser probe inside patient's head (Courtesy: Medtronic Inc.).

This is due to the power of two laser probes (Power: 15 W vs. 12 W) and the directional side firing (SideFire) capability of the NeuroBlate® system.[65] The potential disadvantage of the Visualase® system is the difficulty of changing the laser probe insertion orientation once the cranial anchor is threaded into the skull. The applicator might need to be repositioned in order to compensate for the unacceptable orientation error.[96]

MERLIN

The MERLIN (MRI-Enabled Robotic non-Linear Incisionless Neurosurgery) (Fig. 4) is a robotic system developed in Vanderbilt University[16,23,73] and intended for transforamenal ablation of hippocampus for the treatment of epilepsy. It includes a concentric tube delivery mechanism and a radiofrequency ablation (RFA) probe. The concentric tube delivery system is fabricated in helical shape to fit the long axis of the hippocampus. Based on the corrugated diaphragm theory, the authors developed a 2-DoF pneumatic actuator by combining a helix-shaped bellow and a toroid-shape bellow together. The proposed 2 DoF MR conditional flexible fluidic actuator has the rotation accuracy of 0.018 degree and translation accuracy of 0.013 mm.[23] The helical concentric tube is controlled and deployed in a follow-the-leader fashion to prevent shearing surround tissue by coupling its rotation and translation motion together. A custom designed aiming device is used to provide the entry angle of the docking tube, where the concentric tube is extended to reach the tail of hippocampus. The RFA probe is deployed from the helical concentric tube tip. The concentric tubes and RFA probe is partially retracted step by step such that the whole hippocampus can be ablated. Similar to the commercially available systems, MERLIN is controlled remotely by a surgeon using the intraoperative MRI guidance.

Noteworthy advantage of MERLIN is that it enables nonlinear trajectory (helical shape) to reach the hippocampus through the patient's cheek *via* a natural orifice (i.e. the foramen ovale). Preliminary phantom study shows that the ablation zone can be well predicted based on the concentric tube robot shape and RFA probe insertion depth.[16] The robotic platform has been tested inside a 3T MRI scanner to quantify its MR conditionality with both T1-w and T2-w image sequences. Phantom image signal to noise ratio (SNR) was utilized as the main performance index and the preliminary study show that the maximum SNR reduction is less than 5%. MERLIN could potentially provide a less invasive approach since no additional hole needs to be drilled in the skull. However, more trials need to be performed on animal/human studies to validate the feasibility of the transforamenal approach in the future.

WPI Neurosurgery Robot

The neurosurgery robot developed at Worcester Polytechnic Institute[56] is a piezoelectrically actuated robotic system for MRI-guided precision conformal ablation of brain tumors using an interstitial ultrasound-based thermal ablator probe. To simplify the iterative workflow of MRI-guided interventions that typically require moving the patient inside the scanner for imaging and moving the patient out of the scanner for intervention, this robot is fully-motorized with all the required degree-of-freedom (DOF) to manipulate

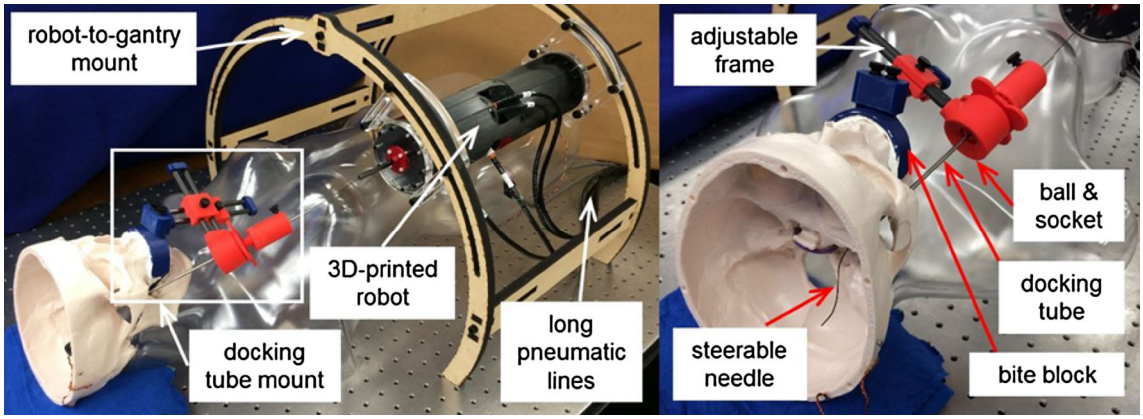

FIGURE 4. Left: Robot actuation unit and aiming device are compactly positioned with a manikin. Right: Close-up view of aiming device and needle.

the ultrasonic ablator. The robot consists of the 5-DOF ablator alignment and positioning module (3-DOF Cartesian motion and 2-DoF rotational remote center of motion) and the 3-DOF ablator driver module (1-DOF insertion motion of the outer tube, as known as cannula, in combination with the 2-DOF ablator rotation and insertion motion). Since the 8-DOF robot can be fully-operated inside the MRI scanner bore during imaging, it has the potential to reduce the procedure time by alleviating the iterative imaging-intervention workflow. The free space positioning accuracy of the system is evaluated with an optical tracking system, demonstrating the root mean square (RMS) error of the tip position to be 1.11 ± 0.43 mm.

The ultrasonic ablator (ACOUSTx, Acoustic MedSystems Inc., Savoy, IL, USA)[33,74,77] is an interstitial high intensity focused ultrasound (iHIFU) based applicator. The ACOUSTx ablator contains 1–4 tubular ultrasound transducers with 5–11 mm length, and is designed to be inserted within a plastic cannula. Figure 5 depicts the exploded view of the 3-DOF ablator driver module. A rigid cannula (component 6) is utilized to guide the ablator into the brain, preventing the ablator from bending during insertion. The cannula is attached to the cannula guide (component 7) and inserted robotically by the linear piezoelectric motor (component 8). The ablator is fixed to the driver through the ablator clamp (component 5), and inserted robotically by the linear piezoelectric directly, and rotated by the rotary piezoelectric through the gears (component 3). The insertion and rotation DOFs of the ablator could control the position and orientation of the directional transducers to generate a desired ablation profile.

The feasibility of the system to perform ablator motion control and thermal ablation treatment is validated through an *ex vivo* tissue study. An *ex vivo* lamb brain tissue was utilized to mimic the human brain and validate the clinical workflow of the robotic brain tumor ablation. The experiment setup is shown in Fig. 6 (left), and the ablator track in the lamb brain is visualized on MR images as illustrated in Fig. 6 (right). The red line represents for the actual US ablator segmented from MRI volume images. The position and orientation errors for the insertion are 0.5 mm and 2.0° respectively. The robot is MR conditional within a 3T Philips Achieva scanner. The robot MR conditionality was characterized by the image SNR and maximum SNR reduction was 2.9 and 10.3% for T1-w and T2-w scan, respectively. In addition, the image distortion caused by the presence of robot was characterized and results indicated that no image warping was observed.[69]

SMA-Actuated Neurosurgical Robot

Ho *et al.* presented MR conditional neurosurgical robot to electrocauterze the tumor within brain in 2012.[39] The robot is constructed by a set of brass segments with the cross-section diameter of 12 mm and actuated by two shape memory alloy (SMA) wires (Fig. 7). SMA has the characteristic of returning to its original shape when heated above the transformation temperature.[39] The hollow core design on the brass segments enables SMA wiring and electric coils for temperature sensor data transmission. SMA mathematical modeling is presented by the authors to characterize the relationship between robot motion and SMA wire temperature. The pulse-width modulation (PWM) method is applied to modulate the SMA wire temperature. Preliminary results show that the robot is able to provide substantial force and torque to reliably operate in a gelatin phantom. The robot creates no significant image distortion and SNR reduction in a 3T MRI scanner.

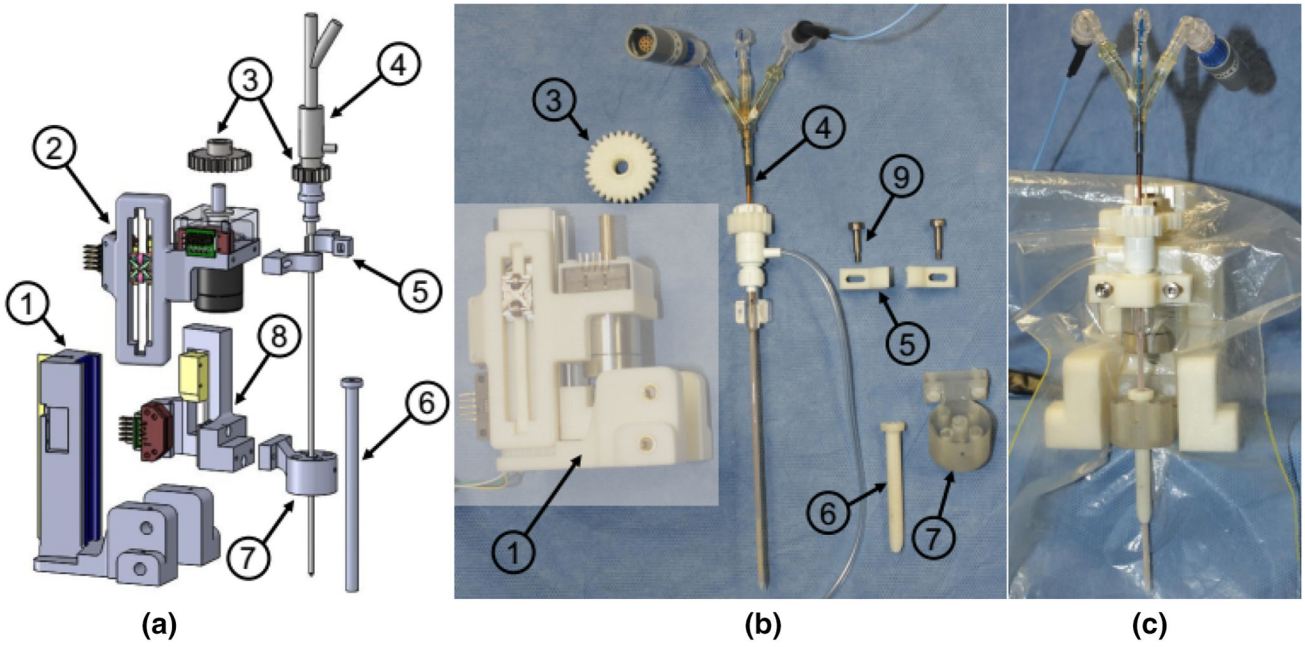

FIGURE 5. 3-DOF ablator driver module that provides 1-DOF insertion motion of the outer tube (as known as cannula) and the 2-DOF ablator rotation and insertion motion.

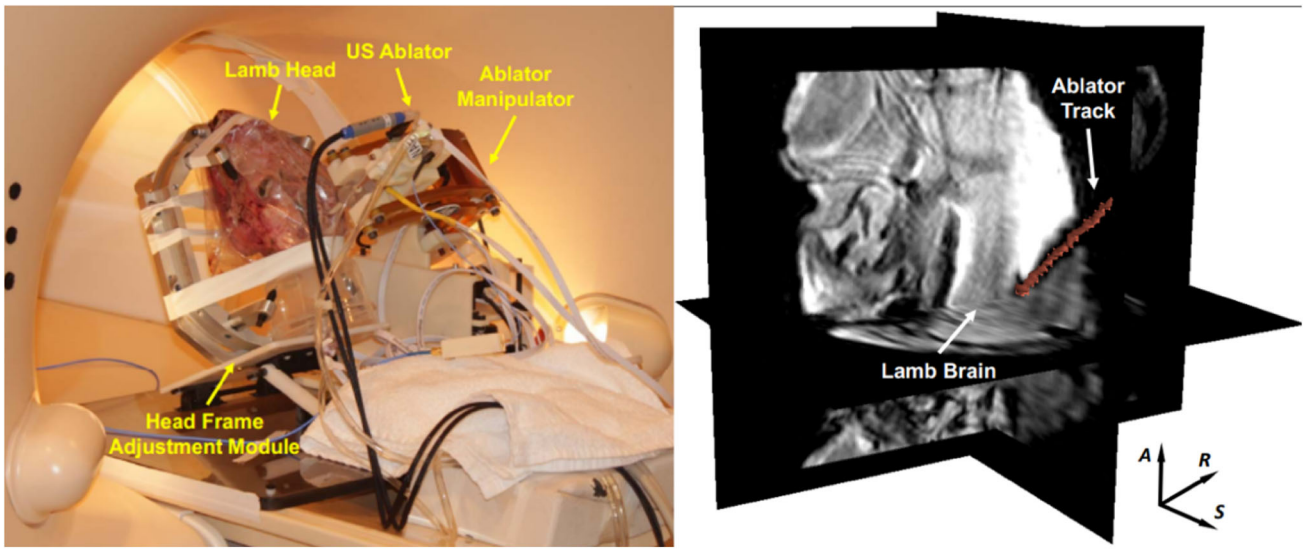

FIGURE 6. (Left) Experiment setup for ultrasound-based thermal ablation on an *ex vivo* lamb brain. (Right) MR image of a representative ablator track in *ex vivo* lamb brain. 3D MR image volume showing the US ablator inserted inside an *ex vivo* lamb brain.

Noteworthy feature of this robot is its dimension and the SMA-based actuation method. Due to the large diameter of each segment, the robot will inevitably cause more damage to the healthy tissue compared to the-state-of-art minimally invasive approaches. The hollow design in the robot design is associated with several challenges in clinical scenarios, including sterilization, direct physical contact between SMA/electric wires and normal healthy brain tissue. Also, the nonlinear, temperature depended and hysteresis characteristics of SMA makes it difficult to achieve fast and accurate control response. The robot is MR conditional within a 3T MRI scanner. In-scanner motion test indicated that the robot was able to operate safely without being affected by the strong magnetic field. The impact of each individual link on the medical image was validated by calculating the SNR. The SNR reduction was about 20% due to the

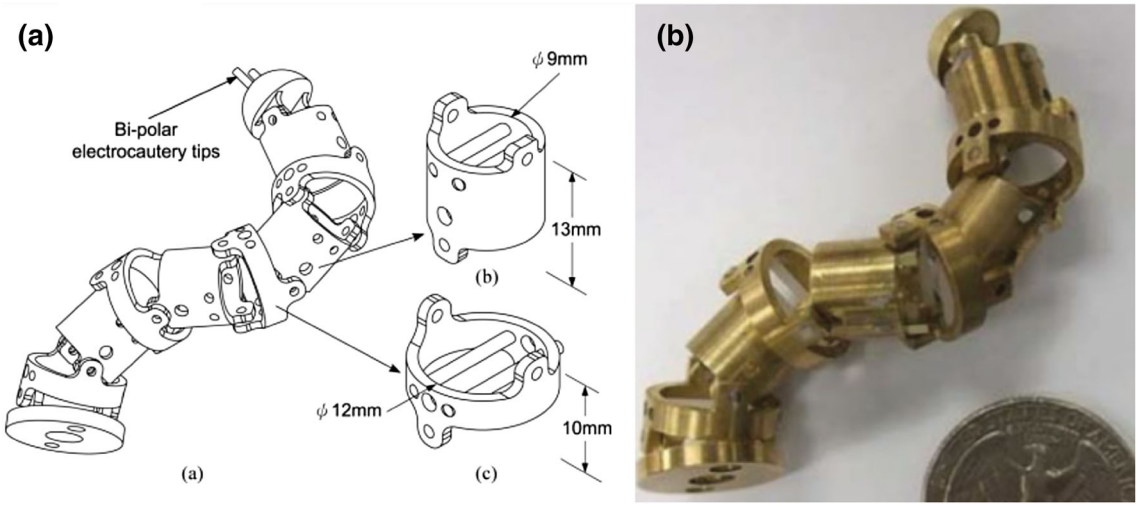

FIGURE 7. SMA robot proposed by Ho *et al.*[39] (a) Schematic diagram of the robot and body segment; (b) robot prototype fabricated with brass.

presence of the robot, however, the SNR was still high enough to identify the links in the MR images. Potential reasons that contribute to the SNR reduction include the eddy current generated due to the varying gradient magnetic field and antenna effect caused by the conductive wires.

Deep Brain Stimulation (DBS) Electrode Placement

Reversible neuro-modulation in the form of DBS, normally using the chronically implanted electrodes, is an established surgical treatment option to alleviate symptoms of Parkinson's disease, dystonia, essential tremor and other neurological disorders when drug therapy is unable to provide the effective treatment.[72] The clinical efficacy of DBS depends on the accurate placement of DBS electrode, which has traditionally relied on awake intraoperative microelectrode recording (MER).[59] The high resolution intraoperative MRI could enhance the accuracy of electrode placement by monitoring its position when patients cannot tolerate awake surgery.[85] In addition, it could also reduce the total procedure time since MER is not necessary in order to confirm the electrode position. In this section, we will review two commercially available MR conditional stereotactic frames for DBS electrode implantation.

Nexframe

Nexframe® (Medtronic, Minneapolis, MN) is a FDA-approved MR-conditional stereotactic aiming system for DBS electrode implantation.[30] It consists of a stereotactic image-guided system, micro-positioner with adjustable z-directional distance, anchoring device for lead stability and microelectrode recording system (Fig. 8). This stereotactic aiming system can be adjusted in the pitch and yaw direction to obtain the desired orientation. To perform the MR-guided electrode placement, general anesthesia and prepping are performed in a room close to an interventional MR scanner. The patient is then transported and placed in the bore of MR scanner and kept immobilized throughout the surgery. Following volumetric scanning to identify the approximate target location and plan the insertion trajectory, the incision is made and burr holes are drilled using an MR conditional cranial drill. Once the dura is open, the Nexframe is mounted over the burr holes on the skull. The final orientation of Nexframe is determined using intraoperative MRI and manually adjusted the trajectory guiding stem.[60,67,86] A ceramic stylet with plastic sheath is manually advanced to the target position in a stepwise motion under real-time MRI guidance. The ceramic stylet is then removed and the electrode is inserted into the sheath. After the electrode position is confirmed by a final high-resolution MR scanning, the stylet is retracted and electrode is anchored to the skull.[45]

The Nexframe has a published mean targeting error of 1.25 mm with a 95% confidence interval of 2.7 mm, compared to the Leksell system's mean error of 1.7 mm with a 95% confidence interval of 3.4 mm.[38] With real-time MR-guidance, the Nexframe is able to account for the error caused by brain shift, which normally occurs when the dura is open. Patient study indicates that the surgical outcomes of Nexframe based approach are comparable to those with the traditional surgical techniques.

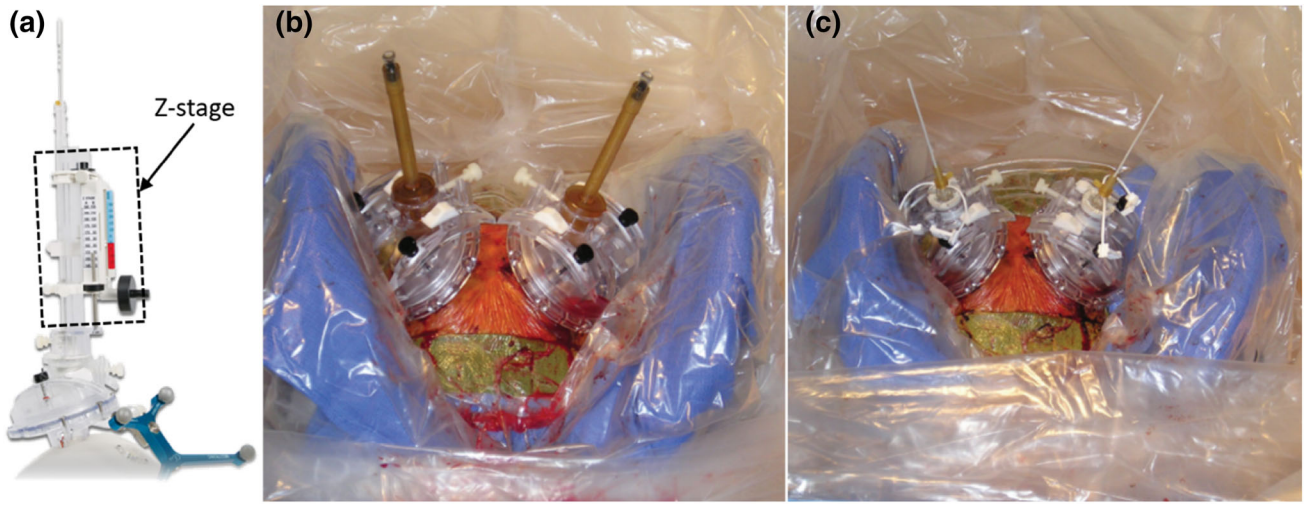

FIGURE 8. (a) stereotactic image guided system with adjustable z-stage[67]; (b, c) alignment stems and electrodes on stereotactic guiding frame.[86]

ClearPoint

ClearPoint® (MRI Interventions, Irvine, CA) is another commercially available system to provide stereotactic guidance for DBS electrode implantation under real-time MRI guidance. It received the FDA approval in June 2010 and was applied in patient procedure in August 2010.[70,81,85] The ClearPoint system consists of a head immobilization frame, a computer workstation, an MR conditional navigation monitor, and a SmartFrame® aiming device (Fig. 9). MR conditional in-room navigation monitor allows the surgeon to visualize the intraoperative image inside the MR room. The SmartFrame® is a 4-DoF (pitch, roll and X and Y translational DoFs),[51] disposable, burr-hole-mounted trajectory aiming frame that enables electrode guidance and insertion during the DBS electrode placement procedure. Pitch/roll ($\pm 33^o$ and $\pm 26^o$ respectively) control the orientation of the trajectory and X–Y linear DoF ($\pm$ 2.5 mm) create parallel trajectories. The dimension of SmartFrame® is small enough such that two frames can be mounted on the skull simultaneously to enable bilateral DBS electrode placement procedures. The workflow is similar to that of Nexframe®. One key difference is that the aiming device could be adjusted remotely by the surgeon through a manual controller, thereby keeping the patient inside the scanner throughout the procedure. Cadaver experiments show that the ClearPoint® has a radial targeting error of 0.2 $\pm$ 0.1 mm with the average procedure time of 88 $\pm$ 14 min; compared to the Nexframe system (error: 0.6 $\pm$ 0.2 mm and procedure time: 92 $\pm$ 12 min).[51]

Noteworthy feature of the ClearPoint® is that it can be used with existing diagnostic MRI suite and compatible with both 1.5T and 3T scanners in a hospital. With real-time intraoperative MR image guidance and remotely control capability, ClearPoint® achieves better targeting accuracy compared to NexFrame system.[38] ClearPoint® system is also versatile and can be used to place laser ablation probe, drug delivery catheter and brain biopsy needle, which could potentially reduce the training cost for the surgeon to master the skill to control manipulate the ClearPoint® system.

neuroArm

neuroArm is a robotic system developed by a group of researchers from University of Calgary in collaboration with Macdonald Dettwiler and Associates (MDA) in 2002 (Fig. 10). It is the first MR conditional neurosurgical robot capable of performing the MR-guided microsurgery. The first patient study with neuroArm was performed by Dr. Sutherland in 2008[92] for tumor removal procedure.

neuroArm consists of two dexterous manipulators and each consists of six manipulation DoF and one tool actuation DoF.[71,93] The manipulators are designed to hold different surgical devices with a maximum payload of 750 g at 200 mm/s speed. The manipulator is fabricated with non-ferromagnetic materials (i.e. titanium, polyetheretherketone and polyoxymethylene) and powered by ultrasonic actuators (Nanomotion, Yokneam, Israel) to meet the MR conditionality requirements. High resolution encoders are assembled at each joint to provide the accurate close loop control and force/torque sensor at the end effectors provide the haptic feedback for a more immersive and realistic surgical experience.[66] The manipulators are mounted on a mobile base and controlled remotely by a surgeon using two modified

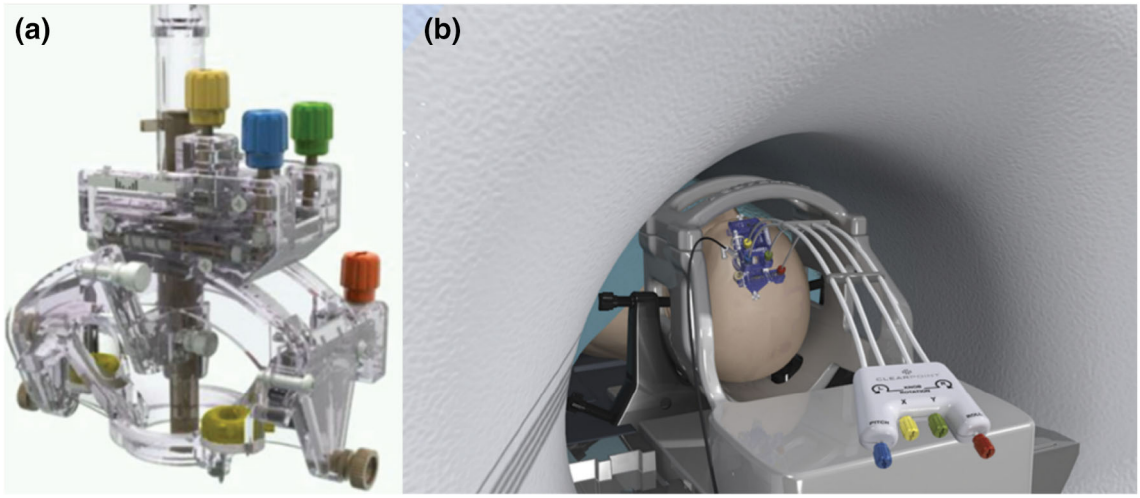

FIGURE 9. (a) 4-DOF SmartFrame® design[85]; (b) Hand controller connected to the SmartFrame® through semirigid rods.[51] This design permits the surgeon to control the trajectory without moving the patient back and forth.

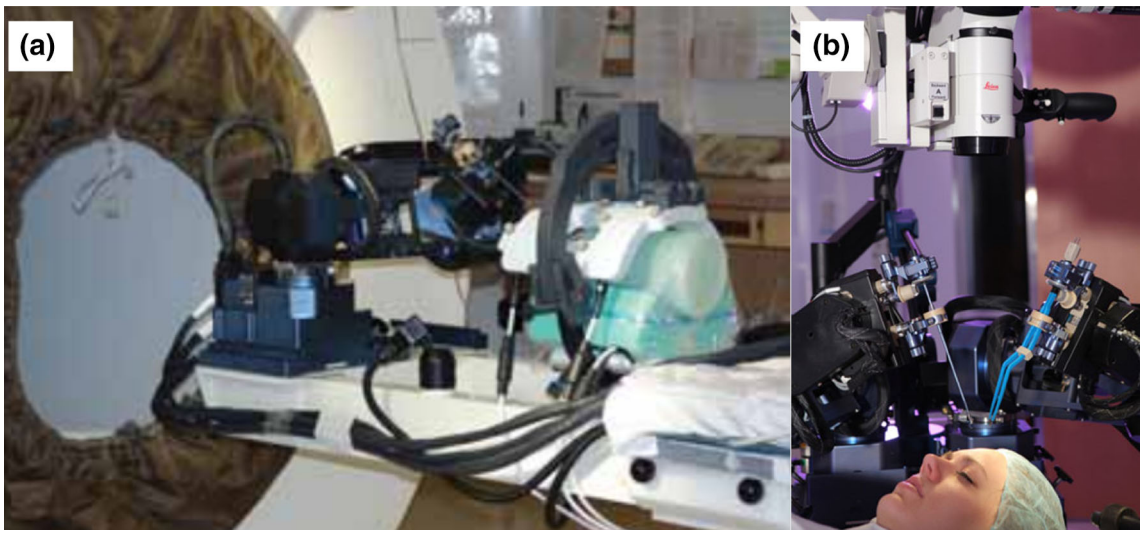

FIGURE 10. neuroArm on the top of extension table for stereotaxy inside the 1.5T MRI room.[93] (a) neuroArm inside the MRI scanner room; (b) The two dexterous manipulators of neuroArm.

Phantom Omni controllers with real-time image from the surgical site.

Animal study in a rodent model show that the overall performances (i.e. procedure time, blood loss and vascular injury) of neuroArm is comparable to the traditional surgical technique (18.5 ± 1.4 min vs. 17.9 ± 2.4 min).[71] However, the mean localization error of neuroArm is better than that of conventional systems (4.35 ± 1.68 mm vs. 10.4 ± 2.79 mm). Noting that an equal performance is found in cadaver studies of implanting a nano-particle in head model with both neuroArm and conventional technique.[71]

Noteworthy features of the neuroArm system is its improved motion precision and targeting accuracy. Despite the expensive cost of the neuroArm platform and lack of high-fidelity haptic feedback, the researchers in neuroArm group pioneered the development of MRI-guided robotic neurosurgery. Noting that the high healthcare cost can also be well justified by the improved surgical outcome and procedure safety, as claimed by Lepski *et al.*[55]

ICH Robot

Recently, the researchers from Vanderbilt University developed a 3-DoF MR conditional robot for intracerebral hemorrhage (ICH) aspiration.[15] The basic components of the real-time MRI-guided robotic system for ICH removal are shown in Fig. 11a. It consists of a robot for actuating the concentric tubes,

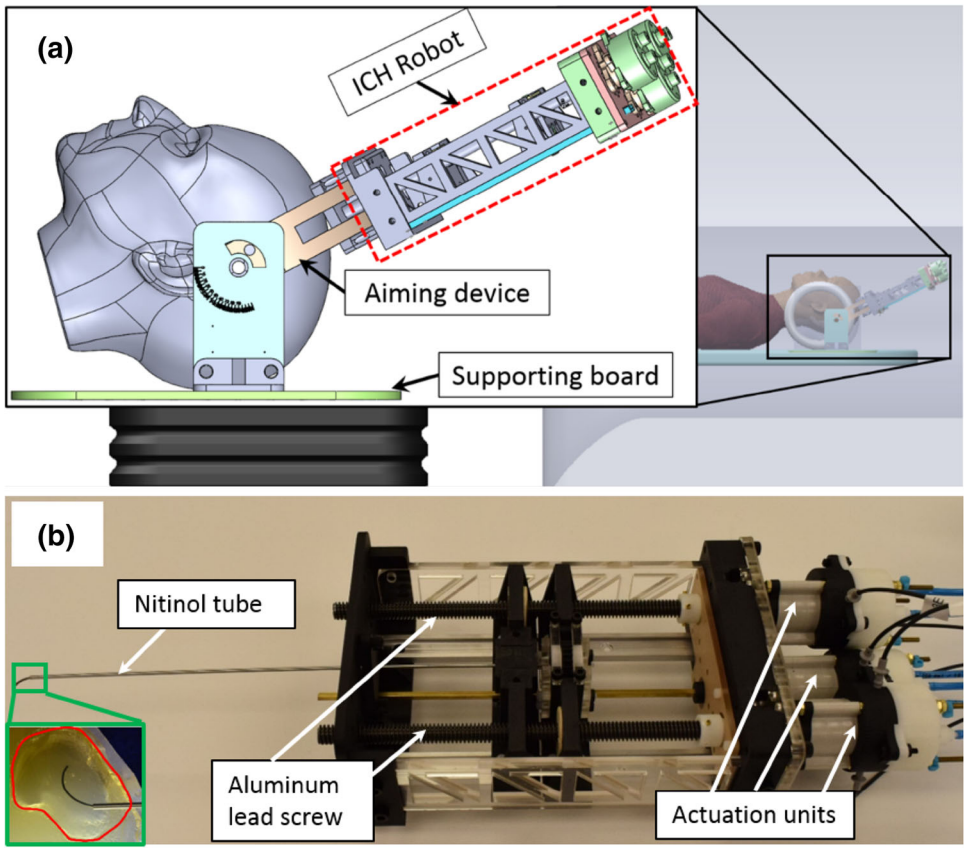

FIGURE 11. (a) Schematic diagram of MR conditional ICH robot integrated with an aiming device inside the MRI scanner; (b) prototype of the MR conditional robot. Left bottom inset shows a close-up of a steerable needle inside a blood clot phantom (red boundary).

combined with an aiming device to initially manipulate the robot at desired orientation. In the envisioned clinical workflow, the patient's head is immobilized with respect to the MR scanner and robot with a head frame or clamp system. A safe entry path to the ICH is specified by the neurosurgeon, then the robot is aligned along the preferred path by the aiming device, and the concentric tubes pass along the path and into the hematoma. Using the real-time MR image generated in the region of interest around the needle tip, the physician will be able to account for brain cavity motion during aspiration process and steer the needle to safely aspirate the hematoma from within.

The MR conditional ICH robot system Fig. 11b consists of a biocompatible actuation unit and uses a mechanical design similar to that of Ref. 7, but different in that it is designed to be MR conditional. Each of the actuators is a novel type of pneumatic Pelton turbine motor, fabricated using a Stratasys Dimension SST 3D printer and equipped with a custom-made optical encoder enabling bi-directional encoding.[10] The robot is fabricated entirely with nonmagnetic materials, e.g. plastic, acrylic, brass, and aluminum. The image quality variation caused by the presence of the robot are characterized inside a 3T Philips MRI room by calculating the SNR under the T1-weighted fast field echo (T1 W-FFE) and T2-weighted turbo spin echo (T2w-TSE) imaging sequences. The results indicate that the robot is MR conditional within the 3T MRI environment with the maximum SNR reduction of 3.2 and 4.9%, respectively.

Noteworthy features of the proposed MR conditional ICH robot is that it has the tip targeting accuracy of 1.26 ± 1.22 mm. The robot could accurately reach the target position by integrating the real-time MR image guidance. *In vitro* ICH evacuation experiment was performed in the gelatin phantom and result indicated that the proposed robot could efficiently (11.3 ml phantom hematoma was aspirated in approximately 9 min) and successfully aspirate the phantom hematoma without causing damage to the surrounding healthy region.[9] This robot is MR conditional within the 3T MRI scanner. The MR conditionality was characterized with the SNR under T1 W-FFE and T2w-TSE imaging sequences with the maximum SNR reduction of 3.2 and 4.9%, respectively.

MR Conditional Biopsy Robot

Ken Masamune *et al.*, developed a 6 DoF MR conditional needle insertion robot in 1995[61] (see Fig. 12). The robot consists of a 3 DoF XYZ stage for target position localization, 2 DoF for orientation control, and a translation DoF for needle feeding. The authors used an isocentric mechanism concept in the rotational latitude DoF design to obtain substantial mechanical safety and design simplicity. Six ultrasonic motors (Shinsei Kogyo, Tokyo, Japan) were used to drive the robot and optical encoders were coupled to each joint for close loop position control. The robot has a dimension of 360 mm × 395 mm × 380 mm, which can be fitted with an open scanner and state-of-the-art close scanner. To operate safely inside the scanner and avoid generating artifacts in MR images, the robot was fabricated with MR conditional materials. The XYZ base, guiding rail and arc were fabricated with polyethylene terephthalate; drive shaft was made out of aluminum; needle insertion and latitude rotation was achieved through rubber gear belts. The screws and bearings were fabricated with polyether ether ketone and ceramic, respectively. The robot was controlled through a personal computer located in the control room and connected to the robot *via* a 7 m shielded cable for data communication.

Noteworthy features of this robot is its accuracy performance. The robot accuracy performance was evaluated in two aspects. Benchtop tests showed that the positioning accuracy was in the order of 10 μm for all joints and backlash was in the order of 100 μm except the depth axis (2.4 mm). Needle targeting test in watermelon was performed under a 0.5T MRI system (MRH-500, Hitachi, Tokyo, Japan). The tip error was within 3.3 mm (x = 1.4 mm, y = 1.5 mm, z = 2.6 mm respectively). The error was believed to be caused by the low image resolution of the MRI scanner. MR-conditionality tests indicated that no image artifact was created in the region of interested when the power is off. The robot was designed for biopsy purpose, but the integration of the biopsy needle with the robot was not covered in the manuscript. The robotic system is MR conditional within a 0.5T Hitachi MRI scanner. No artifacts were been produced due to the presence of the robotic platform. The robot was able to function accurately inside the scanner despite that no comprehensive MR conditionality results were reported.

MR Safe Needle Guidance Robot

Dan Stoianovici *et al.* developed a general MR safe needle guidance robot that could be applied in neurosurgery application.[44,89] The robotic setup consists of 5 DoFs. The robotic manipulator orients the needle-guide with 2 DOFs around the fulcrum point using a novel remote center of motion (RCM) mechanism. The 2 rotation DoFs have the operation range of [− 50, 30]° and [− 40, 40]° respectively. The proposed RCM mechanism provides the high structural stiffness by using a vertically non-collinear joint arrangement and a redundant parallelogram. The two rotational DoFs are driven by the custom designed MR safe pneumatic motor that are located in the actuation module. The RCM sits on top of a passive arm with 3 DoFs which provides the manual adjustment of RCM location. The manual supporting arm is affixed to the sliding channels on the MRI table, which provides an extra translation DoF. The robot will be covered with a sterile bag during the procedure and the only component that needs to be sterilized is the needle-guide module. The robotic platform is able to provide the guidance for needles or devices with the diameter up to 10 mm by constructing the corresponding bore. The robot is entirely built of nonconductive, nonmetallic, and nonmagnetic materials,

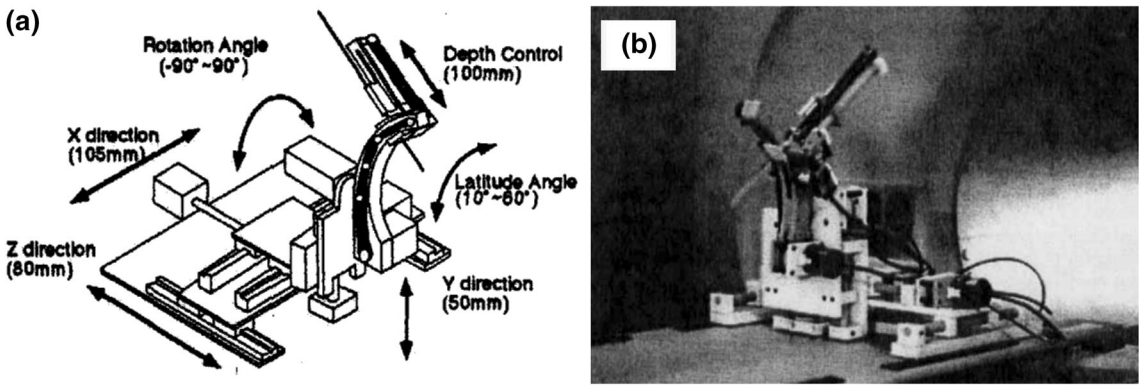

FIGURE 12. The 5 DoF needle insertion robot and the range of motion of each DoF.[61]

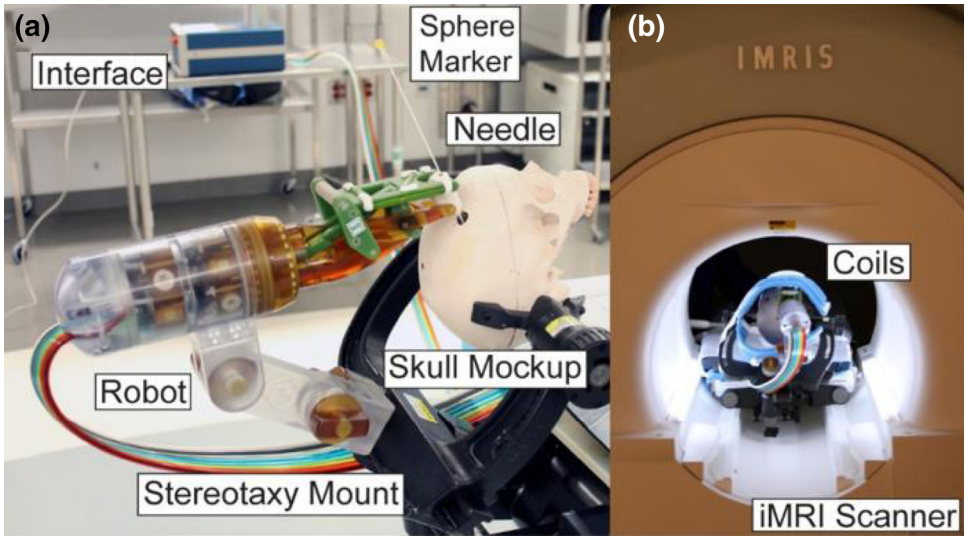

FIGURE 13. Robot and skull (a) on the table and (b) inside the MRI scanner.[44]

TABLE 2. Comparative study of the MR conditional actuation methods.

Actuation method	Advantages	Disadvantages
Piezoelectric motor	Accurate and precise Long lifetime Compact design High bandwidth	MR conditionality issue Expensive
Hydraulic motor	Large power Flexible installation Force control capability	Potential fluid leakage
Pneumatic motor	MR safe with plastic materials High power density Easy to be fabricated with 3D printer Inexpensive	System delay

which include the plastics, rubber, composites, glass, and high-alumina ceramic (Fig. 13).

This robot has been tested extensively in benchtop and in-scanner conditions to validate its performance. The joint space positioning tests indicate that the robot has the accuracy of submillimeter in the two active rotation joints. RCM mechanism is extremely accurate with the average error of 0.136 mm. The robot end effector targeting test in the *in vitro* settings indicate that the robot has the average accuracy and precision of 1.71 and 0.51 mm respectively. Stiffness characterization results show that the robot has the stiffness of 33.38 N/mm axially and 25.53 N/mm laterally. The robot is MR safe and generates minimal SNR change during the image quality test. Surgical workflow of utilizing the proposed robotic platform has been analyzed. The results indicate that the robot is able to hit 12 targets in 97 min. Noteworthy feature of this robotic platform is that it could be used in multiple applications, such as the neurosurgery[44] and bone biopsy.[22]

ACTUATOR AND SENSOR OF MR CONDITIONAL ROBOT

Actuating

The manual-controlled stereotactic aiming devices described in "State-of-the-art Neurosurgical Stereotactic Devices" section have been found to be accurate in most of the clinical applications. However, it requires lengthy training periods to attain the required proficiency to manipulate the aiming device at the desired position and orientation. Robot-assisted devices have the tremendous potential to improve the accuracy and safety during neurosurgeries. In this section, we will review the actuator technologies that can be used to fabricate MR conditional robot for neurosurgery. The characteristics of each actuation method are summarized in Table 2.

Piezoelectric motors, such as HR2-1-N-10 (Nanomotion Inc., Yokneam, Israel) or USM-60N1(Shinsei Kogyo Corp, Tokyo, Japan), have been widely used in MRI-

guided robotic systems due to their accuracy, reliability and self-locking capability.[19,29,48,93] The major limitations of piezoelectric motors are high cost and, most importantly, the need to disconnect the power during image acquisition to prevent image distortion due to magnetic fields caused by the electrical conductors.[29,47] 3T MRI conditionality results show that approximately 40–60% SNR reduction can be observed during the motor power is on.[47] The SNR reduction can be as high as 80% without proper RF shielding.[48] As a result, the intraoperative imaging is normally carried out while the robot is not operating, which could potentially affect the efficiency of surgical workflow. Recent results show that better image quality can be achieved with custom-designed piezo actuator drivers and control method which are not commercially available yet.[28,36]

Alternatively, hydraulic actuations can be used for driving MR conditional robots.[31,32,46] The advantages of hydraulic actuation are high flexibility and absence of electro-magnetic components. The MR conditionality performance of hydraulic actuation purely depends on the materials property since its working principle is electro-magnetically decoupled from MR scanner. The major limitation of hydraulic actuations includes the potential liquid leakage issue due to the nonmetallic materials used in constructing these actuation systems.[31]

Pneumatic actuation is easy to fabricate and also electromagnetically decoupled from MR scanner. Compressed sterile air supplies are available in hospitals. Pneumatic pistons and motors are two major types of MR conditional pneumatic actuation methods.[29,87] Pneumatic piston, fabricated using graphite and glass, can provide accurate linear translational motion but requires additional transmission mechanism to achieve rotational motion. Pneumatic actuators can be fabricated with MR safe plastic materials (i.e. nylon and polyamide) through additive manufacturing. The first MR safe pneumatic actuator was proposed by Stoianovici in 2007 and has been applied in MR conditional robot design.[87,88] Following his pioneering work, a number of MR conditional actuators have been proposed in the past ten years.[4,11,12,17,23,34,35,76,78] One of the major limitation of pneumatic actuation is the system response delay due to long air hose used to connect the air hose and pneumatic motor (0.37 s with a 8 m air hose[18]).

Sensing

The position and force feedback are required to achieve the accurate task space position control and haptic control. The MR conditional force sensors used in MRI-guided interventions have been reviewed in our recent publication.[90] In this paper, we focus on the position sensing technique for MR conditional robot control.

The robot joint space position sensing can be easily achieved through commercially available optical linear and rotatory encoders,[56] which has the resolution of 0.0127 mm and 0.072° respectively. With accurate joint space feedback, robot end effector position can be calculated based on the forward kinematics. However, task space position sensing is often required to compensate tissue deformation, inaccurate kinematic modeling, and robot deformation (i.e. flexible catheters/needles). Hata *et al*. employed an optical tracker (Flash Point, Image-Guided Technologies, Boulder, CO) on the needle-guiding manipulator for MRI-guided ablation therapy.[37] End effector position can be calculated through the homogeneous transformation methods. The major disadvantage of this approach is that it requires constant visual contact between tracking camera and optical markers. Another position tracking approach is the gradient field sensing technique[42] (EndoScout, RobinMedical Systems, Baltimore, MD), which applies 3 orthogonal pick-up coils to calculate position information by measuring the gradient field strength. However, it is not reliable to track the metallic devices since the gradient field linearity is distorted due to the presence of metallic objects.

Visualization of the end effector in MR images is a direct approach to locate its position. There are three fundamental methods of MRI-based tracking: (1) passive tracking; (2) semi-active tracking; and (3) active tracking. Passive tracking relies on the susceptibility artifact of surgical devices inside the patient body or the fiducial markers filled with gadolinium/dysprosium close to the patient body. However, this approach not only requires substantial scanning time to obtain the MR images, but also induces errors in fiducial marker segmentation. Both semi-active and active tracking are performed by mounting a micro RF receiver coil on the surgical device. Different from semi-active tracking coil which couples to the MR scanner wirelessly, active tracking coil is connected to the scanner through a coaxial cable. This design enables it to be turned off when the coil is located in the region of interested to obtain better target image quality.[14] Compared to the passive tracking approach, RF coil could achieve sub-millimeter accuracy at approximately 40 Hz update rate.[13,14,79,100] However, a sophisticated tracking sequence needs to be implemented in the MRI control console to process the signals from RF coils. In addition, sterilization remains challenging when the tracking coils are integrated with minimally surgical devices.

FUTURE PERSPECTIVES

This section presents the key challenges from the authors' perspective that need to be overcome for the development of MR conditional neurosurgical robot. It comprises the following four aspects: actuator, sensor, image guidance and design method.

Actuator Technology

One of the main challenges in designing and constructing compact MR conditional robot is the actuation unit. Precision and price are the two major concerns in prototyping the MR conditional robots. From the discussion in "Actuator and Sensor of MR Conditional Robot" section piezo actuator and pneumatic motors are the most common actuators, which are also among the extremes in terms of actuation precision and affordability characteristic. However, actuating the piezo motor not only degrades the image quality but also raises safety concerns due to magnetic field induced heating. Pneumatic actuation, on the other hand, provides an affordable and safe alternative to prototype MR conditional robots in the initial stages. But the reliability and lifecycle of pneumatic motors need to be rigorously investigated, especially for those are fabricated with plastic materials.

Sensor Technology

MR conditional position sensing techniques in the robot task space remains an interesting and relevant topic. From the authors' perspective, sterilization and integration with surgical device are the two main challenges to advance MR conditional sensor design. MRI active tracking coil demonstrates promising results among the existing tracking technologies due to its small dimension, accurate tracking resolution and high update rate. Recent study has validated the position tracking performance of a brachytherapy stylet integrated with a micro active tracking coil in the animal study and human study.[14] Further research needs to be conducted on the integration of micro tracking coils with neurosurgical devices (e.g., ablation fiber, catheter, electrode, or micro tube *etc.*). Besides the fast MR conditional position sensing, lack of accurate force feedback is believed to be one of the main barriers to improve the widespread adoption of neurosurgical robots, particularly in the robot remote control process. Fiber bragg grating (FBG) force sensing technique has been integrated with MR conditional surgical devices and shown promising results.[90] Beyond this, other force sensing techniques need to be studied given that they could meet the requirements of miniaturization, sterilization, and MR conditionality. For instance, force sensing technique based on shape deflection and static modeling in continuum robot precludes the integration of additional force sensor. Effective utilization of the limited sensor feedback data is another active research topic. Anrea *et al.* proposed the kinematics-based method for contact force detection and contact location in the continuum medical robots.[3] Hence, there is strong reason to encourage further studies in sensor feedback data recording, processing, and ultimately integration with robot control.

Image Guidance

MRI is increasingly used in the preoperative planning and postoperative evaluation of neurosurgical procedures. Real-time intraoperative MR image provides valuable information during therapies, such as medical device localization, temperature map visualization, and ablation outcome monitoring. However, the intraoperative images are normally obtained at low resolution due to the limited scanning time during surgery and the presence of additional medical instruments. Kwok *et al.* proposed an iterative update scheme by registering the high resolution preoperative anatomical model with intraoperative image, which could obtain intraoperative surgical image feedback with improved visualization results.[50,53] However, fast registration of intraoperative images to the preoperative anatomical model requires high performance computing architecture and efficient registration algorithms. By having an accurate intraoperative target anatomic model, virtual fixtures can also be implemented to constraint medical devices' motion within the predefined region to improve the surgical safety.

Design Methodologies

Current commercially available neurosurgical stereotactic tools require straight linear trajectories. However, human anatomical structures do not necessarily follow straight lines. Furthermore, tissue deformation and motion lead to significant challenges when using these rigid tools on dynamic living tissue. Concentric tube robotics is an attractive and feasible solution in neurosurgical robot end effector design to address these limitations. Concentric tube manipulators enable access to target sites while avoiding critical function areas of the brain which is hard to reach using rigid straight devices. Concentric tube based neurosurgical treatment has been successfully validated in simulation and phantom studies.[16] However, the integration of concentric tube robotics with the existing surgical devices is challenging. For example, inserting a laser ablation probe or biopsy needle into the con-

centric tubes could significantly change the curved-tube shape and stiffness, making them complex and non-intuitive for accurate control. Precise fabrication of a concentric tube robot according to patient-specific requirements, for example tube mechanical property, diameter, curvature and length curved portion, is an active research topic.

An interesting phenomenon is that all the commercialized neurosurgical stereotactic aiming devices are passive mechanisms while the robotic prototypes developed in the laboratory setting are partially or fully active. Besides the neuroArm, no active devices are being commercialized by major medical device vendors. At present, surgeons are hesitant to try fully active robots in neurosurgical applications. Potential reasons are (1) robotic neurosurgery is not suitable for all the patients; (2) lack of tactile feedback in terms of tissue texture and density; (3) large physical dimensions and therefore cumbersome to use in the MR room; (4) difficulty in integration with existing surgical workflow and protocols; (5) challenges in sterilization, and (6) cost issues. Addressing these in the robot design process could potentially encourage the widespread adoption of MR conditional robots in neurosurgeries.

Robot Technology

A tele-operative robot that combines the benefits of the surgeon's experience and the motor's accuracy is becoming a promising tool to perform the neuro surgical procedures. Performing the procedure teleoperatively could lead to improved treatment outcomes, reduced recovery time, shorten hospital stay, reduced invasiveness, and reduced the morbidity rates. Although recent results indicate that there is a need for haptic feedback in the tele-operative surgical robot, there is still no consensus in terms of when force sensing is necessary or beneficial in the specific surgical scenarios. Lots of multidimensional haptic sensors have been developed based on strain gauges, piezoelectric effects, capacitive effects, and optical measurements, while they are still unable to satisfy the requirement in the neurosurgical field due to the large dimension and difficulty to install at the robot end effector. Another challenge is display device design for haptic feedback. There are three types of haptic display devices, including handhold pentype haptic display devices, wearable haptic display devices, and desktop haptic display devices. Noting that the transmission reducers are not allowed to use in the electric motor due to the backdrivability requirement. Therefore the current haptic display devices are only able to provide no more than 3N force to the human operator. To overcome the disadvantage of the electrical motor, some researchers proposed the passive force feedback method based on magnetorheological fluid, which generates large passive force on the human hand. There is an urgent need to design an effective method to produce large and accurate haptic display for surgical robot teleoperation.[43,75]

CONCLUSIONS

MR conditional stereotactic devices for neurosurgery is a vibrant and growing research topic in the field of medical robotics. In this paper, we present an overview of the state-of-the-art stereotactic devices that are being used for MRI-guided neurosurgery. This paper details the review and comparative study of existing MR conditional actuators and encoders. Potential challenges and future directions in terms of actuator, sensor, image guidance and robot design are detailed in this paper.

The robotic stereotactic devices in neurosurgeries provide precise, reliable, and dexterous manipulation of surgical devices. Advanced robotic stereotactic system design could enhance the patient's safety and reduce pain and discomfort. MR conditional robotics needs to incorporate new techniques to reduce its cost and improve surgeon's familiarity to gain wide acceptance. We expect the future of MR conditional stereotactic robot to be bright.

ACKNOWLEDGMENTS

Yue Chen acknowledge Eric Barth and Robert Webster for their comments that greatly improved the manuscript. Yue Chen also thank Sang-Eun 'Sam' Song for the suggestions on MRI terminology.

CONFLICT OF INTEREST

None to declare.

REFERENCES

[1]Adler, Jr, J. R., S. D. Chang, M. J. Murphy, J. Doty, P. Geis, and S. L. Hancock. The Cyberknife: a frameless robotic system for radiosurgery. *Stereotact. Funct. Neurosurg.* 69(1–4):124–128, 1997.

[2]ASTM-F2503. Standard practice for marking medical devices and other items for safety in the magnetic resonance environment. www.astm.org.

[3]Bajo, A., and N. Simaan. Kinematics-based detection and localization of contacts along multisegment continuum robots. *IEEE Trans. Robot.* 28(2):291–302, 2012.

[4]Bosboom, D. G. H., J. J. Fütterer, and J. Bosboom. Motor system, motor, and robot arm device comprising the same. Google Patents, 2016.
[5]Bown, S. Phototherapy of tumors. *World J. Surg.* 7(6):700–709, 1983.
[6]Brandmeir, N. J., J. McInerney, and B. E. Zacharia. The use of custom 3D printed stereotactic frames for laser interstitial thermal ablation. *Neurosurg. Focus* 41(4):E3, 2016.
[7]Burgner, J., P. J. Swaney, R. A. Lathrop, K. D. Weaver, and R. J. Webster. Debulking from within: a robotic steerable cannula for intracerebral hemorrhage evacuation. *IEEE Trans. Biomed. Eng.* 60(9):2567–2575, 2013.
[8]Chan, F., *et al.* Image-guided robotic neurosurgery—an in vitro and in vivo point accuracy evaluation experimental study. *Surg. Neurol.* 71(6):640–647, 2009.
[9]Chen, Y., I. S. Godage, S. Sengupta, C. L. Liu, K. D. Weaver, and E. J. Barth. MR-compatible steerable needle robot for intracerebral hemorrhage removal. *Int. J. Comput. Assist. Radiol. Surg.* 2018. https://doi.org/10.1007/s11548-018-1854-z.
[10]Chen, Y., I. S. Godage, Z. T. H. Tse, R. J. Webster, and E. J. Barth. Characterization and control of a pneumatic motor for MR-conditional robotic applications. *IEEE/ASME Trans. Mechatron.* 22(6):2780–2789, 2017.
[11]Chen, Y., K.-W. Kwok, and Z. T. H. Tse. An MR-conditional high-torque pneumatic stepper motor for MRI-guided and robot-assisted intervention. *Ann. Biomed. Eng.* 42(9):1823–1833, 2014.
[12]Chen, Y., C. D. Mershon, and Z. T. H. Tse. A 10-mm MR-conditional unidirectional pneumatic stepper motor. *IEEE/ASME Trans. Mechatron.* 20(2):782–788, 2015.
[13]Chen, Y., T. T. Zion, W. Wang, R. Y. Kwong, W. G. Stevenson, and E. J. Schmidt. Intra-cardiac MR imaging & MR-tracking catheter for improved MR-guided EP. *J. Cardiovasc. Magn. Reson.* 17(1):P237, 2015.
[14]Chen, Y., *et al.* Design and fabrication of MR-tracked metallic stylet for gynecologic brachytherapy. *IEEE/ASME Trans. Mechatron.* 21(2):956, 2016.
[15]Chen, Y., *et al.* An MRI-compatible robot for intracerebral hemorrhage removal. In: 2017 Design of Medical Devices Conference, pp. V001T08A019-V001T08A019, 2017. American Society of Mechanical Engineers..
[16]Chen, Y., *et al.* Treating epilepsy via thermal ablation: initial experiments with an MRI-guided concentric tube robot. In: 2017 Design of Medical Devices Conference, pp. V001T02A002-V001T02A002, 2017. American Society of Mechanical Engineers.
[17]Chen, Y., *et al.* Robotic system for MRI-guided focal laser ablation in the prostate. *IEEE/ASME Trans. Mechatron.* 22(1):107–114, 2017.
[18]Chen, Y., *et al.* MRI guided robotically assisted focal laser ablation of the prostate using canine cadavers. *IEEE Trans. Biomed. Eng.* 2017.
[19]Chinzei, K., and K. Miller. Towards MRI guided surgical manipulator. *Med. Sci. Monit.* 7(1):153–163, 2001.
[20]Chung, Y. C., J. L. Duerk, A. Shankaranarayanan, M. Hampke, E. M. Merkle, and J. S. Lewin. Temperature measurement using echo-shifted FLASH at low field for interventional MRI. *J. Magn. Reson. Imaging* 9(1):138–145, 1999.
[21]Clarke, R. The structure and functions of the cerebellum examined by a new method. *Brain* 45, 1908.
[22]Cleary, K., *et al.* Robotically assisted long bone biopsy under MRI imaging: workflow and preclinical study. *Acad. Radiol.* 25(1):74–81, 2018.
[23]Comber, D. B., J. E. Slightam, V. R. Gervasi, J. S. Neimat, and E. J. Barth. Design, additive manufacture, and control of a pneumatic MR-compatible needle driver. *IEEE Trans. Robot.* 32(1):138–149, 2016.
[24]Eljamel, M. Robotic application in epilepsy surgery. *Int. J.Med. Robot. Comput. Assist. Surg.* 2(3):233–237, 2006.
[25]Eljamel, M. S. Robotic applications in neurosurgery. *Medical Robotics* 1(1):11–22, 2008.
[26]Fan, X., D. W. Roberts, J. D. Olson, C. Li, and K. D. Paulsen. Image updating for brain deformation compensation: cross-validation with intraoperative ultrasound. In: Medical Imaging 2018: Image-Guided Procedures, Robotic Interventions, and Modeling. International Society for Optics and Photonics, vol. 10576, p. 105760S.
[27]Fankhauser, H., *et al.* Robot for CT-guided stereotactic neurosurgery. *Stereotact. Funct. Neurosurg.* 63(1–4):93–98, 1994.
[28]Fischer, G. S., G. Cole, and H. Su. Approaches to creating and controlling motion in MRI. In: Annual International Conference of the IEEE Engineering in Medicine and Biology Society, EMBC, pp. 6687–6690, 2011. IEEE.
[29]Fischer, G. S., A. Krieger, I. Iordachita, C. Csoma, L. L. Whitcomb, and G. Fichtinger. MRI compatibility of robot actuation techniques–a comparative study. In: International Conference on Medical Image Computing and Computer-Assisted Intervention, pp. 509–517, 2008. Springer.
[30]Franck, J. I., *et al.* Instrument guidance for stereotactic surgery. Google Patents 2001.
[31]Gassert, R., R. Moser, E. Burdet, and H. Bleuler. MRI/fMRI-compatible robotic system with force feedback for interaction with human motion. *IEEE/ASME Trans. Mechatron.* 11(2):216–224, 2006.
[32]Gassert, R., *et al.* A 2-DOF fMRI compatible haptic interface to investigate the neural control of arm movements. In: Proceedings 2006 IEEE International Conference on Robotics and Automation, 2006 (ICRA 2006), pp. 3825–3831, 2006. IEEE.
[33]Ghoshal, G., *et al.* Ex-vivo and simulation comparison of multi-angular ablation patterns using catheter-based ultrasound transducers. In: Energy-Based Treatment of Tissue and Assessment VII, vol. 8584, p. 85840Y, 2013. International Society for Optics and Photonics.
[34]Groenhuis, V., and S. Stramigioli. Laser-cutting pneumatics. *IEEE/ASME Trans. Mechatron.* 21(3):1604–1611, 2016.
[35]Guo, Z., T. Lun, Y. Chen, H. Su, D. Chan, and K. Kwok. Novel design of an MR-safe pneumatic stepper motor for MRI-guided robotic interventions. In: Proceedings of the Hamlyn Symposium on Medical Robotics, 2016: Imperial College London and the Royal Geographical Society London. http://hamlyn.doc.ic.ac.uk/hsmr/programme/symposium-proceedings.
[36]Hao, S., A. Camilo, G. A. Cole, H. Nobuhiko, C. M. Tempany, and G. S. Fischer. High-field MRI-compatible needle placement robot for prostate interventions. *Stud. Health Technol. Inform.* 163:623, 2011.
[37]Hata, N., J. Tokuda, S. Hurwitz, and S. Morikawa. MRI-compatible manipulator with remote-center-of-motion control. *J. Magn. Reson. Imaging* 27(5):1130–1138, 2008.

[38]Henderson, J. M., K. L. Holloway, S. E. Gaede, and J. M. Rosenow. The application accuracy of a skull-mounted trajectory guide system for image-guided functional neurosurgery. *Comput. Aided Surg.* 9(4):155–160, 2004.
[39]Ho, M., A. McMillan, J. M. Simard, R. Gullapalli, and J. P. Desai. Towards a meso-scale SMA-actuated MRI-compatible neurosurgical robot. *IEEE Trans. Robot.* 2011(99):1, 2011.
[40]Hongo, K., *et al.* NeuRobot: telecontrolled micromanipulator system for minimally invasive microneurosurgery—preliminary results. *Neurosurgery* 51(4):985–988, 2002.
[41]Housepian, E. M., and J. L. Pool. The accuracy of human stereoencephalotomy as judged by histological confirmation of roentgenographic localization. *J. Nerv. Mental Dis.* 130(6):520–525, 1960.
[42]Hushek, S., *et al.* Initial clinical experience with a passive electromagnetic 3D locator system. In: 5th Interventional MRI Symposium, 2004, no. 605.
[43]Jerbic, B., G. Nikolic, D. Chudy, M. Svaco, and B. Sekoranja. Robotic application in neurosurgery using intelligent visual and haptic interaction. *Int. J. Simul. Model.* 14(1):71–84, 2015.
[44]Jun, C., *et al.* MR safe robot assisted needle access of the brain: preclinical study. *J. Med. Robot. Res.* 3(01):1850003, 2018.
[45]Khan, F. R., and J. M. Henderson. Deep brain stimulation surgical techniques. In: Handbook of Clinical Neurology, Vol. 116, edited by K. Levin, and P. Chauvel. Amsterdam: Elsevier, 2013, pp. 27–37.
[46]Kim, D., E. Kobayashi, T. Dohi, and I. Sakuma. A new, compact MR-compatible surgical manipulator for minimally invasive liver surgery. In: International Conference on Medical Image Computing and Computer-Assisted Intervention, pp. 99–106, 2002. Springer.
[47]Krieger, A., *et al.* Development and preliminary evaluation of an actuated MRI-compatible robotic device for MRI-guided prostate intervention. In: IEEE International Conference on Robotics and Automation (ICRA), pp. 1066–1073, 2010. IEEE.
[48]Krieger, A., *et al.* Development and evaluation of an actuated MRI-compatible robotic system for MRI-guided prostate intervention. *IEEE/ASME Trans. Mechatron.* 18(1):273–284, 2013.
[49]Kwoh, Y. S., J. Hou, E. A. Jonckheere, and S. Hayati. A robot with improved absolute positioning accuracy for CT guided stereotactic brain surgery. *IEEE Trans. Biomed. Eng.* 35(2):153–160, 1988.
[50]Kwok, K.-W., *et al.* Interfacing fast multi-phase cardiac image registration with MRI-based catheter tracking for MRI-guided electrophysiological ablative procedures. *Am Heart Assoc* 2014.
[51]Larson, P. S., P. A. Starr, G. Bates, L. Tansey, R. M. Richardson, and A. J. Martin. An optimized system for interventional magnetic resonance imaging-guided stereotactic surgery: preliminary evaluation of targeting accuracy. *Oper. Neurosurg.* 70(suppl_1):ons95–ons103, 2011.
[52]Le Roux, P. D., H. Das, S. Esquenazi, and P. J. Kelly. Robot-assisted microsurgery: a feasibility study in the rat. *Neurosurgery* 48(3):584–589, 2001.
[53]Lee, K.-H., Z. Guo, G. C. Chow, Y. Chen, W. Luk, and K.-W. Kwok. GPU-based proximity query processing on unstructured triangular mesh model. In: IEEE International Conference on Robotics and Automation (ICRA), pp. 4405–4411, 2015. IEEE.
[54]Leksell, L. The stereotactic method and radiosurgery of the brain. *Acta Chir. Scand.* 102:316–319, 1951.
[55]Lepski, G., *et al.* MRI-based radiation-free method for navigated percutaneous radiofrequency trigeminal rhizotomy. *J. Neurol. Surg. Part A* 76(02):160–167, 2015.
[56]Li, G., *et al.* Robotic system for MRI-guided stereotactic neurosurgery. *IEEE Trans. Biomed. Eng.* 62(4):1077, 2015.
[57]Lieberman, I. H., *et al.* Bone-mounted miniature robotic guidance for pedicle screw and translaminar facet screw placement: part I—technical development and a test case result. *Neurosurgery* 59(3):641–650, 2006.
[58]Louw, D. F., T. Fielding, P. B. McBeth, D. Gregoris, P. Newhook, and G. R. Sutherland. Surgical robotics: a review and neurosurgical prototype development. *Neurosurgery* 54(3):525–537, 2004.
[59]Machado, A., A. R. Rezai, B. H. Kopell, R. E. Gross, A. D. Sharan, and A. L. Benabid. Deep brain stimulation for Parkinson's disease: surgical technique and perioperative management. *Mov. Disord.* 21(S14):S247–S258, 2006.
[60]Martin, A. J., *et al.* Placement of deep brain stimulator electrodes using real-time high-field interventional magnetic resonance imaging. *Magn. Reson. Med.* 54(5):1107–1114, 2005.
[61]Masamune, K., *et al.* Development of an MRI-compatible needle insertion manipulator for stereotactic neurosurgery. *J. Image Guid Surg* 1(4):242–248, 1995.
[62]McRobbie, D. W., E. A. Moore, and M. J. Graves. MRI from Picture to Proton. Cambridge: Cambridge University Press, 2017.
[63]Medvid, R., *et al.* Current applications of MRI-guided laser interstitial thermal therapy in the treatment of brain neoplasms and epilepsy: a radiologic and neurosurgical overview. *Am. J. Neuroradiol.* 2015.
[64]Miga, M. I., *et al.* Modeling of retraction and resection for intraoperative updating of images. *Neurosurgery* 49(1):75–85, 2001.
[65]Mohammadi, A. M., and J. L. Schroeder. Laser interstitial thermal therapy in treatment of brain tumors–the NeuroBlate System. *Expert Rev. Med. Devices* 11(2):109–119, 2014.
[66]Motkoski, J. W., and G. R. Sutherland. Progress in neurosurgical robotics. In: Intraoperative Imaging and Image-Guided Therapy, edited by F. A. Jolesz. New York: Springer, 2014, pp. 601–612.
[67]Nexframe Deep Brain Stimulation for Movement Disorders. http://professional.medtronic.com/pt/neuro/dbs-md/prod/index.htm#tabs-3.
[68]Norred, S. E., and J. A. Johnson. Magnetic resonance-guided laser induced thermal therapy for glioblastoma multiforme: a review. *BioMed Res. Int.*, vol. 2014, 2014.
[69]Nycz, C. J., *et al.* Mechanical validation of an MRI compatible stereotactic neurosurgery robot in preparation for pre-clinical trials. In: IEEE/RSJ International Conference on Intelligent Robots and Systems (IROS), pp. 1677–1684, IEEE 2017.
[70]Ostrem, J. L., *et al.* Clinical outcomes using ClearPoint interventional MRI for deep brain stimulation lead placement in Parkinson's disease. *J. Neurosurg.* 124(4):908–916, 2016.
[71]Pandya, S., J. W. Motkoski, C. Serrano-Almeida, A. D. Greer, I. Latour, and G. R. Sutherland. Advancing neurosurgery with image-guided robotics. *J. Neurosurg.* 111(6):1141–1149, 2009.

[72]Perlmutter, J. S., and J. W. Mink. Deep brain stimulation. *Annu. Rev. Neurosci.* 29:229–257, 2006.
[73]Pitt, E. B., D. B. Comber, Y. Chen, J. S. Neimat, R. J. Webster, and E. J. Barth. Follow-the-leader deployment of steerable needles using a magnetic resonance-compatible robot with stepper actuators. *J. Med. Devices* 10(2):020945, 2016.
[74]Prakash, P., V. A. Salgaonkar, E. C. Burdette, and C. J. Diederich. Hepatic ablation with multiple interstitial ultrasound applicators: initial ex vivo and computational studies. In: Energy-Based Treatment of Tissue and Assessment VI, vol. 7901, p. 79010R, 2011, International Society for Optics and Photonics.
[75]Qin, H., A. Song, Z. Gao, Y. Liu, and G. Jiang. A multi-finger interface with MR actuators for haptic applications. *IEEE Trans. Haptics* 11(1):5–14, 2018.
[76]Sajima, H., H. Kamiuchi, K. Kuwana, T. Dohi, and K. Masamune. MR-safe pneumatic rotation stepping actuator. *J. Robot. Mechatron.* 24(5):820–827, 2012.
[77]Scott, S. J., *et al.* Interstitial ultrasound ablation of tumors within or adjacent to bone: contributions of preferential heating at the bone surface. In: Energy-Based Treatment of Tissue and Assessment VII, vol. 8584, p. 85840Z, 2013. International Society for Optics and Photonics.
[78]Secoli, R., M. Robinson, M. Brugnoli, and F. Rodriguez y Baena. A low-cost, high-field-strength magnetic resonance imaging–compatible actuator. *Proc. Inst. Mech Eng. Part H* 229(3):215–224, 2015.
[79]Sengupta, S., S. Tadanki, J. C. Gore, and E. B. Welch. Prospective real-time head motion correction using inductively coupled wireless NMR probes. *Magn. Reson. Med.* 72(4):971–985, 2014.
[80]Shen, W., J. Gu, and E. Milios. Robotic neurosurgery and clinical applications. In: International Conference on Proceedings of Intelligent Mechatronics and Automation, pp. 114-119, 2004. IEEE.
[81]Sidiropoulos, C., *et al.* Intraoperative MRI for deep brain stimulation lead placement in Parkinson's disease: 1 year motor and neuropsychological outcomes. *J. Neurol.* 263(6):1226–1231, 2016.
[82]Skopec, M. A primer on medical device interactions with magnetic resonance imaging systems, Feb. 4, 1997, CDRH Magnetic Resonance Working Group, US Department of Heatlh and Human Services. *Food Drug Admin Center Device Radiol Health Updated May* 23:17, 1997.
[83]Smith, J. A., J. Jivraj, R. Wong, and V. Yang. 30 Years of neurosurgical robots: review and trends for manipulators and associated navigational systems. *Ann. Biomed. Eng.* 44(4):836–846, 2016.
[84]Spiegel, E. A., H. T. Wycis, M. Marks, and A. Lee. Stereotaxic apparatus for operations on the human brain. *Science* 106(2754):349–350, 1947.
[85]Starr, P. A., L. C. Markun, P. S. Larson, M. M. Volz, A. J. Martin, and J. L. Ostrem. Interventional MRI–guided deep brain stimulation in pediatric dystonia: first experience with the ClearPoint system. *J. Neurosurg.* 14(4):400–408, 2014.
[86]Starr, P. A., A. J. Martin, J. L. Ostrem, P. Talke, N. Levesque, and P. S. Larson. Subthalamic nucleus deep brain stimulator placement using high-field interventional magnetic resonance imaging and a skull-mounted aiming device: technique and application accuracy. *J. Neurosurg.* 112(3):479–490, 2010.
[87]Stoianovici, D., A. Patriciu, D. Petrisor, D. Mazilu, and L. Kavoussi. A new type of motor: pneumatic step motor. *IEEE/ASME Trans. Mechatron.* 12(1):98–106, 2007.
[88]Stoianovici, D., *et al.* MRI-safe robot for endorectal prostate biopsy. *IEEE/ASME Trans. Mechatron.* 19(4):1289–1299, 2014.
[89]Stoianovici, D., *et al.* Multi-imager compatible, MR safe, remote center of motion needle-guide robot. *IEEE Trans. Biomed. Eng.* 65(1):165–177, 2018.
[90]Su, H., *et al.* Fiber optic force sensors for MRI-guided interventions and rehabilitation: a review. *IEEE Sens. J.* 17(7):1952, 2017.
[91]Sugiyama, K., T. Sakai, I. Fujishima, H. Ryu, K. Uemura, and T. Yokoyama. Stereotactic interstitial laser-hyperthermia using Nd-YAG laser. *Stereotact. Funct. Neurosurg.* 54(1–8):501–505, 1990.
[92]Sutherland, G. R., I. Latour, and A. D. Greer. Integrating an image-guided robot with intraoperative MRI. *IEEE Eng. Med. Biol. Mag.* 27(3):59–65, 2008.
[93]Sutherland, G. R., I. Latour, A. D. Greer, T. Fielding, G. Feil, and P. Newhook. An image-guided magnetic resonance-compatible surgical robot. *Neurosurgery* 62(2):286–293, 2008.
[94]Taylor, R., *et al.* A steady-hand robotic system for microsurgical augmentation. *Int. J Robot. Res.* 18(12):1201–1210, 1999.
[95]The future of surgery. http://gelookahead.economist.com/slideshow/the-future-of-surgery/.
[96]Tovar-Spinoza, Z., D. Carter, D. Ferrone, Y. Eksioglu, and S. Huckins. The use of MRI-guided laser-induced thermal ablation for epilepsy. *Child's Nerv. Syst.* 29(11):2089–2094, 2013.
[97]Tyc, R., and K. J. Wilson. Laser surgery/cancer treatment: real-time interactivity enhances interstitial brain tumor therapy. *Laser* 5:01, 2010.
[98]Varma, T., and P. Eldridge. Use of the NeuroMate stereotactic robot in a frameless mode for functional neurosurgery. *Int. J. Med. Robot. Comput. Assist. Surg.* 2(2):107–113, 2006.
[99]Visualase MRI-Guided Laser Ablation. http://www.medtronic.com/us-en/healthcare-professionals/products/neurological/laser-ablation/visualase.html (2017-07-10).
[100]Wang, W., *et al.* Evaluation of an active magnetic resonance tracking system for interstitial brachytherapy. *Med. Phys.* 42(12):7114–7121, 2015.
[101]Zamorano, L., Q. Li, S. Jain, and G. Kaur. Robotics in neurosurgery: state of the art and future technological challenges. *Int J. Med. Robot. Comput. Assist. Surg.* 1(1):7–22, 2004.
[102]Zimmermann, M., R. Krishnan, A. Raabe, and V. Seifert. Robot-assisted navigated endoscopic ventriculostomy: implementation of a new technology and first clinical results. *Acta Neurochir.* 146(7):697–704, 2004.